NEOPLASIA
www.neoplasia.com
Volume 23 Number 5 May 2021 pp. 515–528

Original Research

Synergistic effect of Chloroquine and Panobinostat in ovarian cancer through induction of DNA damage and inhibition of DNA repair ☆, ☆☆

María Ovejero-Sánchez [a,b,c]; Rogelio González-Sarmiento [a,b,c,*]; Ana Belén Herrero [a,b,c,*]

[a] Institute of Biomedical Research of Salamanca (IBSAL), Salamanca, Spain
[b] Molecular Medicine Unit, Department of Medicine, University of Salamanca, Salamanca, Spain
[c] Institute of Molecular and Cellular Biology of Cancer (IBMCC), University of Salamanca-CSIC, Salamanca, Spain

ABSTRACT

Ovarian cancer (OC) is the deadliest gynecologic malignancy, which is mainly due to late-stage diagnosis and chemotherapy resistance. Therefore, new and more effective treatments are urgently needed. The in vitro effects of Panobinostat (LBH), a histone deacetylase inhibitor that exerts pleiotropic antitumor effects but induces autophagy, in combination with Chloroquine (CQ), an autophagy inhibitor that avoid this cell survival mechanism, were evaluated in 4 OC cell lines. LBH and CQ inhibited ovarian cancer cell proliferation and induced apoptosis, and a strong synergistic effect was observed when combined. Deeping into their mechanisms of action we show that, in addition to autophagy modulation, treatment with CQ increased reactive oxygen species (ROS) causing DNA double strand breaks (DSBs), whereas LBH inhibited their repair by avoiding the correct recruitment of the recombinase Rad51 to DSBs. Interestingly, CQ-induced DSBs and cell death caused by CQ/LBH combination were largely abolished by the ROS scavenger N-Acetylcysteine, revealing the critical role of DSB generation in CQ/LBH-induced lethality. This role was also manifested by the synergy found when we combined CQ with Mirin, a well-known homologous recombination repair inhibitor. Altogether, our results provide a rationale for the clinical investigation of CQ/LBH combination in ovarian cancer.

Neoplasia (2021) 23, 515–528

Keywords: Chloroquine, Panobinostat, autophagy, ROS, DNA damage andrepair, homologous recombination

Introduction

Ovarian cancer (OC) is one of the most common gynecologic malignancies and it has the highest mortality rate among them, nearly 185 000 annual deaths worldwide [1]. This high mortality is mainly due to the asymptomatic growth of the tumor that results in its diagnosis in advanced stages [2]. In addition, relapse of disease is common after surgery and standard platinum-based chemotherapy [3,4], and also after further treatments with different chemotherapeutic agents [5]. Therefore, there is a clear need to develop new therapeutic strategies. One of these strategies should be efficient drug combinations that could overcome resistances and improve ovarian cancer survival.

Histone deacetylase inhibitors (HDACi) represent promising agents in cancer treatment [6]. The first of these compounds approved by the FDA was SAHA in 2006 for the treatment of cutaneous T-cell lymphoma, followed by Romidepsin in 2009, Belinostat in 2014 and Panobinostat (LBH) in 2015 for the treatment of different hematological malignancies [7]. Many others HDACi are currently in clinical trials for the treatment of several cancers. All these molecules inhibit HDACs, critical regulators of gene expression that deacetylate different histones acting as transcriptional repressors [8]. The inhibition of HDACs promotes transcriptional activation of multiple genes that are silenced in human tumors [9]. Moreover, HDACi have been shown to exert pleiotropic antitumor effects; they induce the expression of proapoptotic genes, cause cellular differentiation and/or cell cycle arrest

* Corresponding authors.
E-mail addresses: gonzalez@usal.es (R. González-Sarmiento), anah@usal.es (A.B. Herrero).

☆ Abbreviations: CQ, Chloroquine; DSB, double strand breaks; HDACi, histone deacetylase inhibitors; OC, ovarian cancer; LBH, Panobinostat; ROS, reactive oxygen species.

☆☆ Declaration of competing interest: The authors declare no conflict of interest. The funders had no role in the design of the study; in the collection, analyses, or interpretation of data; in the writing of the manuscript, or in the decision to publish the results.

Received 17 February 2021; received in revised form 8 April 2021; accepted 10 April 2021

https://doi.org/10.1016/j.neo.2021.04.003

[6,10,11] and impair DNA repair [12–16]. HDACi also promote autophagy, but this effect instead of exerting antitumor effects has been proposed as a potential mechanism of resistance to these drugs; autophagy might recycle proteins to generate energy in an attempt to survive stressful conditions generated by the treatment [17]. This is the reason why some researchers have analyzed the effect of the combination of HDACi and other proautophagy drugs with autophagy inhibitors, such as Chloroquine (CQ), and have found synergistic effects in some tumor cell lines, such as breast, colon, leukemic and neuroblastoma cell lines [18–23].

CQ was originally discovered and used to treat malaria, and subsequently it was used as an anti-inflammatory agent to treat inflammatory diseases [24]. CQ is a weak base and therefore it can raise the pH of cellular compartments. This led to the assumption that CQ blocks the autophagic flux by increasing the lysosomal pH, which promotes the inhibition of resident hydrolases. However, a recent report has shown that CQ mainly inhibits autophagy by impairing autophagosome fusion with lysosomes rather than by affecting the acidity of this organelle [25]. Some clinical trials have shown that CQ enhance the potential of combinatorial anticancer therapies by increasing tumor cell death [26], although it remains unclear whether this is really due to autophagy inhibition [27,28]. In fact, it has recently been suggested that the ability of CQ to inhibit autophagy by blocking autophagolysosome formation may not be the only mechanism by which it exerts antitumor effect [27,29].

In this study, we analyzed the effect of one HDACi, LBH, and of CQ and their combination in ovarian cancer cells. We show that CQ increases reactive oxygen species (ROS) which causes DNA double strand breaks (DSBs), whereas LBH inhibits the repair of these lethal lesions by affecting the recruitment of the recombinase Rad51 to DSBs (graphical abstract). These results provide an explanation, together with the modulation of autophagy, for the strong synergistic effect that we observed in ovarian cancer cell lines treated with a combination of these drugs.

Materials and methods

Cell lines and culture conditions

The ovarian cancer cell lines (OCCLs) IGROV-1, OVCAR-8, SK-OV-3 and A2780 were acquired from American Type Culture Collection (ATCC) (OVCAR-8, SK-OV-3), European Collection of Authenticated Cell Cultures (ECACC) (A2780) and Merck Millipore (IGROV-1). Multiple myeloma cell line JJN3-HR was previously constructed in our group [12]. IGROV-1, A2780 and JJN3-HR were cultured in RPMI 1640 medium (Gibco) supplemented with 10% heat-inactivated fetal bovine serum (FBS) (Gibco) and 1% penicillin/streptomycin (Gibco). SK-OV-3 and OVCAR-8 were cultured in Dulbecco's modified Eagle's medium (DMEM) (Gibco) supplemented with 10% FBS and 1% penicillin/streptomycin. All cells were incubated at 37°C in a 5% CO_2 atmosphere. The presence of mycoplasma was routinely checked with MycoAlert kit (Lonza) and only mycoplasma-free cells were used in the experiments.

Reagents

Chloroquine (CQ) and N-Acetylcysteine (NAC) were purchased from Sigma-Aldrich, Mirin and Bafilomycin A1 (Baf) were obtained from MedChemExpress, and Panobinostat (LBH) was provided by Novartis Pharmaceuticals.

Cell proliferation assay

OCCLs were seeded into 96-well plates ($4 \bullet 10^3$ cells/mL) and were treated with different concentrations of Chloroquine (10, 25, 50, 75, 100 and 125 μM) or Panobinostat (10, 25, 50, 75, 100 and 150 nM) for 24, 48 or 72 h. Cell proliferation was determined using 3-(4,5-dimethylthiazol-2-yl)-2,5-diphenyl-2H-tetrazolium bromide (MTT) (Sigma-Aldrich). MTT was dissolved in PBS (5 mg/mL) and 10 μL of this salt per well was added to cells. After 1 h of incubation, medium was aspirated, and formazan crystals were dissolved in DMSO (100 μL/well). Absorbance was measured at 570 nm in a plate reader (Ultra Evolution, Tecan). The half maximal inhibitory concentration (IC50) was calculated using GraphPad Prism 8.

Cell cycle analysis

OCCLs were treated with Panobinostat or Chloroquine, fixed in 70% ethanol and stored at 4 °C for later use. Cells were rehydrated with PBS, stained with 50 μg/mL propidium iodide (PI) (Sigma-Aldrich) and treated overnight with 100 μg/mL RNase A in the dark (Sigma-Aldrich). Cell cycle profiles were then analyzed by flow cytometry using BD Accuri C6 Plus Flow Cytometer (BD Biosciences). Data were analyzed with BD Accuri C6 Software.

Apoptosis assay

OCCLs were treated with Chloroquine, NAC and/or Panobinostat, Bafilomycin A1 and/or Panobinostat, and Mirin and/or Chloroquine, for 72 h and then stained with FITC Apoptosis Detection Kit CE (Immunostep) according to the manufacturer's guidelines. Apoptotic cells were determined using BD Accuri C6 Plus Flow Cytometer. The synergism of the combination was quantified using Compusyn Software (ComboSyn, Inc) which is based on the Chou-Talalay method [58] and calculates a combination index (CI) with the following interpretation: $CI > 1$: antagonistic effect; $CI = 1$: additive effect; $CI < 1$ synergistic effect.

Western blot

Cells were resuspended in lysis buffer (50 mM Tris, 130 mM NaCl, 1 mM EDTA, 1% Triton X-100) containing protease inhibitors (Complete, Roche Applied Science, Indianapolis), and protein concentration was measured using the Bradford assay (BioRad). Protein samples (50 μg/lane) were subjected to SDS-PAGE and transferred to PVDF membranes (Millipore). After blocking, membranes were incubated with antibodies against the following proteins: LC3B (1:1000, NB600-1384, Novus Biologicals), Beclin-1 (1:1000, 3738S, Cell signaling), p62 (1:1000, ab109012, abcam) and β-actin (1:10000, Sigma-Aldrich). β-actin was used for loading control. Horseradish peroxidase linked-sheep (antimouse) (NXA931, GE Healthcare) or -goat (antirabbit) (AP307P, Millipore) were used as secondary antibodies at a 1:10000 dilution. Immunoblots were incubated for 1h at room temperature and developed using enhanced chemiluminescence western blotting detection reagents (Thermo Fisher Scientific). Protein expression levels were calculated using ImageJ software.

Detection of reactive oxygen species (ROS) generation

The production of intracellular ROS was determined by DCFH-DA staining using flow cytometry. For short times, OCCLs were seeded at 250,000 cells/well in 6-well plates, incubated for 24 h and then stained with 5 μM DCFH-DA (Sigma-Aldrich) in serum-free medium for 30 min in darkness. After this incubation, performed at 37°C in 5% CO_2, cells were treated with different concentrations of Chloroquine (25, 50 μM), Panobinostat (25, 50 nM) or NAC (15 mM) for 15 min. For long times, OCCLs were seeded at 250,000 cells/well, incubated for 24 h and treated with Chloroquine (25, 50 μM) and/or Panobinostat (25, 50 nM). After that, cells were stained with 5 μM DCFH-DA in serum-free medium for 30 min in darkness (37°C in 5% CO_2). ROS generation was then analyzed using BD Accuri C6 Plus Flow Cytometer.

Immunofluorescence

OCCLs were plated on round glass coverslips (12 mm diameter) (250,000 cells/well in 6-well plates) and after 24 h of culture, cells were treated with Chloroquine, NAC and/or Panobinostat for 48 or 72 h. Then, cells were fixed with 4% paraformaldehyde for 10 min, permeabilized using 0.5% Triton X-100 (Boehringer Mannheim) in PBS for 10 min, blocked in 10% BSA in PBS for 30 min and incubated with phospho-H2AX antibody (1:1000, 05-636, Sigma-Aldrich) and/or Rad51 antibody (1:1000, PC130, Sigma-Aldrich) or LC3B (1:200, NB600-1384, Novus Biologicals) for 1h 30min. After washing, coverslips were incubated with fluorescent secondary antibodies (1:400, Alexa Fluor 488 goat antimouse IgG and/or Alexa Fluor 594 antirabbit, Molecular Probes, Invitrogen) for 1h. DAPI (dihydrochloride of 4', 6-diamidino-2-phenylindole, Roche) was used to visualize the nuclei. Mowiol reagent (Calbiochem) was used to fix preparations on slides. Cells were then analyzed by confocal microscopy (63x) using a LEICA SP5 microscope DMI-6000V model coupled to a LEICA LAS AF software computer.

Homologous recombination (HR) functional assay

SK-OV-3 cell line was transfected with 1 μg of pHR plasmid linearized by digestion with NheI [30]. G418 was added at 500 μg/mL 72 h post-transfection and stable pools were obtained after 3 wk of selection. To measure HR efficiency in stable pools, cells (SK-OV-3 and JJN3) were first preincubated with different concentrations of Panobinostat (5, 7 or 10 nM) for 24 h. Then, 10^6 cells were cotransfected with 5µg of a plasmid that express I-SceI and 0.5 µg of pDsRed-N1 to correct for differences in transfection efficiencies. Transfections were performed using the Amaxa Cell Line Nucleofector Kit V and Amaxa Nucleofector device (Lonza). Programs used were V-005 for SK-OV-3 cell line and T-016 for JJN3 cell line. After transfection, cells were incubated again with the same concentration of Panobinostat for 48 h. Green (EGFP) and Red (DsRed) fluorescence were measured by flow cytometry using BD Accuri C6 Plus Flow Cytometer. HR efficiency was calculated as the ratio of GFP+ to DsRed+ cells.

Statistical analysis

Differences between the results obtained from treated and nontreated cells were assessed for statistical significance using Student's unpaired 2 tailed t-test with IBM SPSS Statistics for Windows version 25.0 (IBM Corp.). ANOVA with Tukey's posthoc test was used when more than 2 groups were compared. Data are presented as mean ± standard deviations. Statistical significance was concluded for values of $P \leq 0.05$.

Results

Chloroquine inhibits proliferation, induces apoptosis and blocks autophagy in ovarian cancer cell lines

The effect of CQ on the proliferation of ovarian cancer cells was evaluated at different concentrations of the drug in 4 OCCLs. We found that treatment with CQ inhibited cell proliferation in a dose- and time-dependent manner in all the cell lines analyzed (Fig. 1A) with IC50 values that ranged from 12.31 µM for A2780 up to 29.05 µM for IGROV-1. To characterize CQ antiproliferative activity, a cell cycle study was performed. Flow cytometry analysis showed that cell cycle profiles were similar in treated/untreated cells at the conditions assayed. A slight accumulation in G0/G1 phase was observed in some cell lines at 24 h that only reached significance in A2780 cell line (*P*-value < 0.05) (Figs. 1B and S1). In addition, a slight increase in the percentage of the sub-G0 population was observed in IGROV-1, OVCAR-8 and SK-OV-3 cell lines; however, a strong and significant increase in the sub-G0 population was found in A2780 cell line after 72 h of treatment (*P*-value < 0.05) (Fig. 1B). To determine whether the cytotoxic effect of CQ was due to the induction of apoptosis, ovarian cancer cells were treated with variable concentrations of the drug, stained with Annexin V-PI, and analyzed by flow cytometry. The results showed that CQ induced apoptosis in a dose-dependent manner, with A2780 being the most sensitive cell line (Fig. 1C).

Chloroquine is a well-known autophagy inhibitor [25], therefore we also analyzed the expression of autophagy-related proteins in OCCLs at different times post treatment. The levels of LC3-II and Beclin-1 increased after CQ treatment (Fig. 1D) in all the cell lines tested. p62 levels also increased in all cell lines except for IGROV-1, probably due to their resistance to CQ. All these results suggest a blockage of the autophagy process [25,27]. To confirm this hypothesis, we performed immunofluorescence assays for LC3B detection. We observed a clear accumulation of autophagosomes in the cytoplasm of the 4 OCCLs (Figure S2).

Panobinostat inhibits proliferation and induces G2/M cell cycle arrest, apoptosis and autophagy

Next, we studied the effect of Panobinostat (LBH) on the proliferation of OCCLs. A dose- and time-dependent effect was observed in the 4 cell lines analyzed, being OVCAR-8 the most sensitive to the HDAC inhibitor (Fig. 2A). An analysis of the cell cycle profiles after LBH treatment revealed that this drug caused an accumulation of cells in G2/M phase in the most sensitive cell lines (SK-OV-3, OVCAR-8) (Figures S2, *P*-value<0.05) and a strong increase in the percentage of death cells, as determined by the quantification of sub-G0 population (Fig. 2B). A dose-dependent induction of apoptosis after treatment with LBH was demonstrated by Annexin-V labeling (Fig. 2C).

HDAC inhibitors have been described to induce autophagy by a variety of mechanisms [31–34]. To investigate whether LBH modulates autophagy in OC cells the levels of autophagy-related proteins were analyzed by western blot. A decrease in p62 protein levels (except for the A2780 cell line) together with an increment of Beclin-1 (in OVCAR-8, IGROV-1 and A2780 cell lines) and LC3B-I were detected after treatment with the drug (Fig. 2D), indicating an induction of autophagy. Interestingly, cotreatment with CQ inhibited LBH-mediated decline in p62 levels (Figure S4), in agreement with a previous report in breast cancer cells [19].

Combination of Panobinostat and Chloroquine synergistically induces cell death in OCCLs

Next, we compared the effect of the combination of LBH and CQ with these agents in monotherapy in the 4 OCCLs. When cells were treated with a combination of CQ (20 μM) and Panobinostat (20 nM) we observed that cell viability was much lower than the observed with each drug alone (Fig. 3). To investigate a putative synergistic effect, we used different doses and maintained a constant ratio. The combination indices (CIs), calculated with the Compusyn software, were below 1 in all OCCLs analyzed, revealing a synergistic interaction between the 2 drugs (Fig. 3). The synergism of the double combination was stronger in OVCAR-8 and A2780 than in the other 2 cell lines since they exhibited very low CIs.

Reactive oxygen species (ROS) generation plays a critical role in CQ/LBH-induced lethality

HDAC inhibitors and CQ are known to exert pleiotropic effects in the cells, which might contribute to their cytotoxicity and to the observed synergism. One of these effects is ROS generation that has been demonstrated in some models [18,35–41]. To determine whether CQ and/or LBH increase ROS generation in OCCLs cells were treated with different concentrations

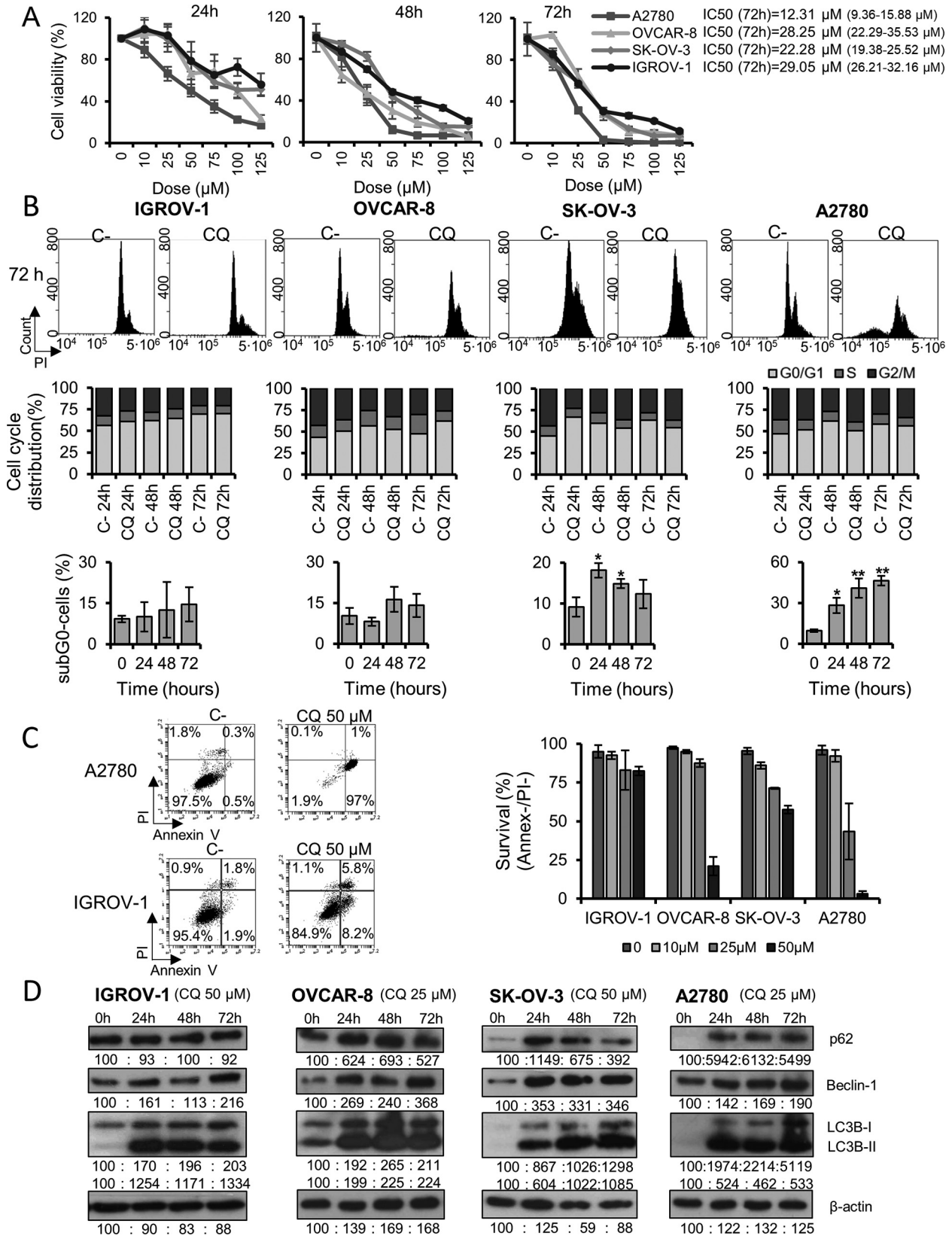

Fig. 1. Effect of Chloroquine in proliferation, cell cycle distribution, apoptosis and autophagy-related proteins in OCCLs. (A) Cell viability after treatment with the indicated doses of CQ for 24, 48 and 72 h. (B) Top panel, cell cycle profile after CQ treatment (50 μM) for 72 h. Middle panel, cell cycle distribution of OCCLs after CQ treatment (50 μM) for 24, 48 and 72 h compared to untreated cells excluding the sub-G0 population. Bottom panel, percentage of death cells after 24, 48 or 72 h of treatment with 50 μM CQ (C) Effect of 72 h CQ-treatment (10, 25 and 50 μM) on apoptosis in OCCLs. D) Time-response of autophagy-related proteins (Beclin-1, LC3B, p62) after CQ treatment (25 or 50 μM). β-actin was used as a loading control. Protein levels were quantified using ImageJ and are indicated. Values were normalized with those corresponding to 0 h that were taken as 100. C-: negative control (untreated cells). Data are the mean of 3 independent experiments. Error bars represent the SD ($^{**}P < 0.01$, $^{*}P < 0.05$).

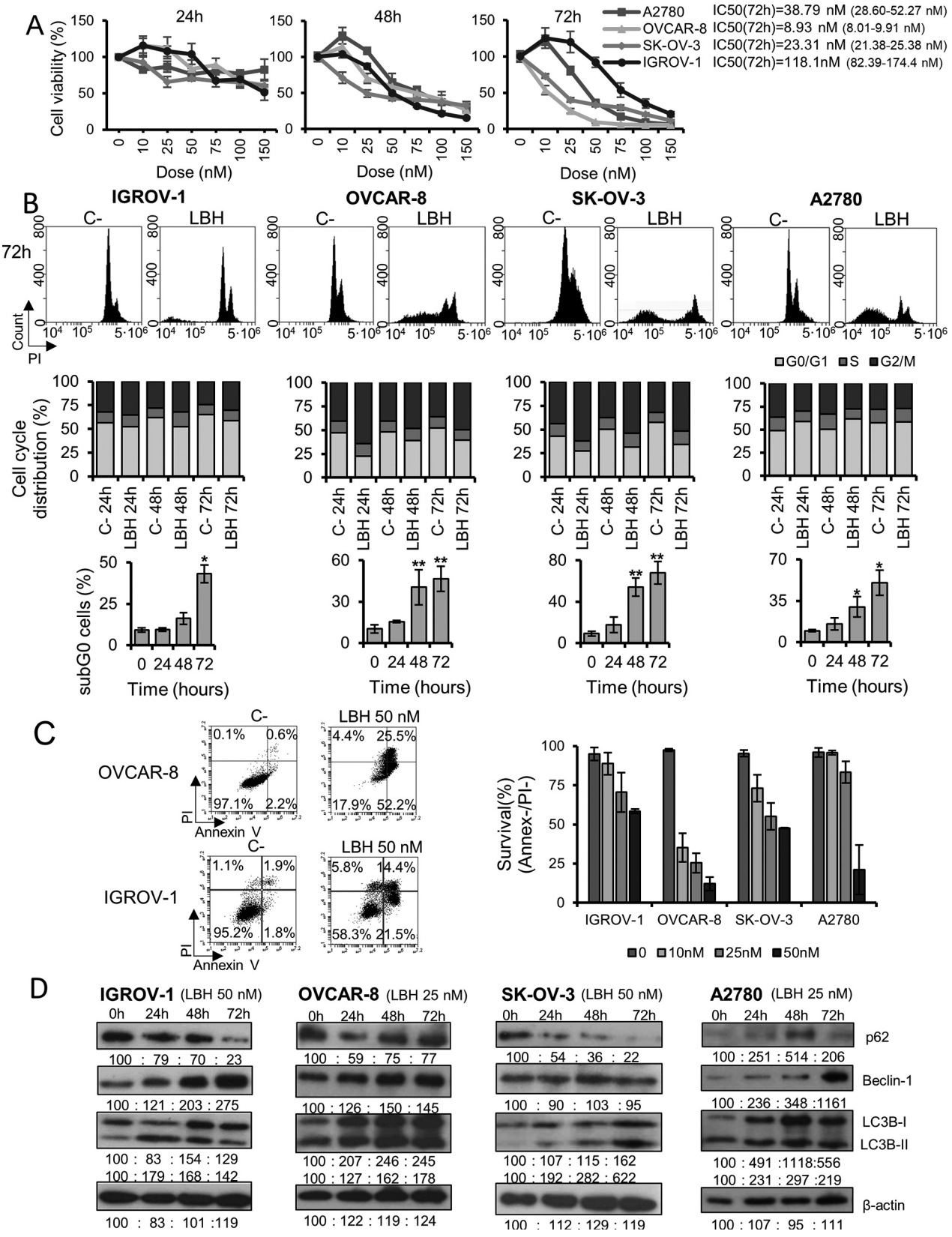

Fig. 2. Effect of Panobinostat in proliferation, cell cycle distribution, apoptosis and autophagy-related proteins in OCCLs. A) Cell viability after treatment with the indicated doses of LBH for 24, 48 and 72 h. B) Top panel, cell cycle profile after LBH treatment (50 nM) for 72 h. Middle the panel, cell cycle distribution of OCCLs after LBH treatment (50 nM) for 24, 48 and 72 h compared with untreated cells excluding the sub-G0 population. Bottom panel, percentage of death cells after 24,48 or 72 h of treatment with 50 nM LBH. C) Effect of 72 h LBH-treatment (10, 25 and 50 nM) on apoptosis in OCCLs. D) Time-response of autophagy-related proteins (Beclin-1, LC3B, p62) after LBH treatment (25 or 50 nM). β-actin was used as a loading control. Protein levels were quantified using ImageJ and are indicated. Values were normalized with those corresponding to 0 h that were taken as 100. C-: negative control (untreated cells). Data are the mean of 3 independent experiments. Error bars represent the SD ($^{**}P < 0.01$, $^{*}P < 0.05$).

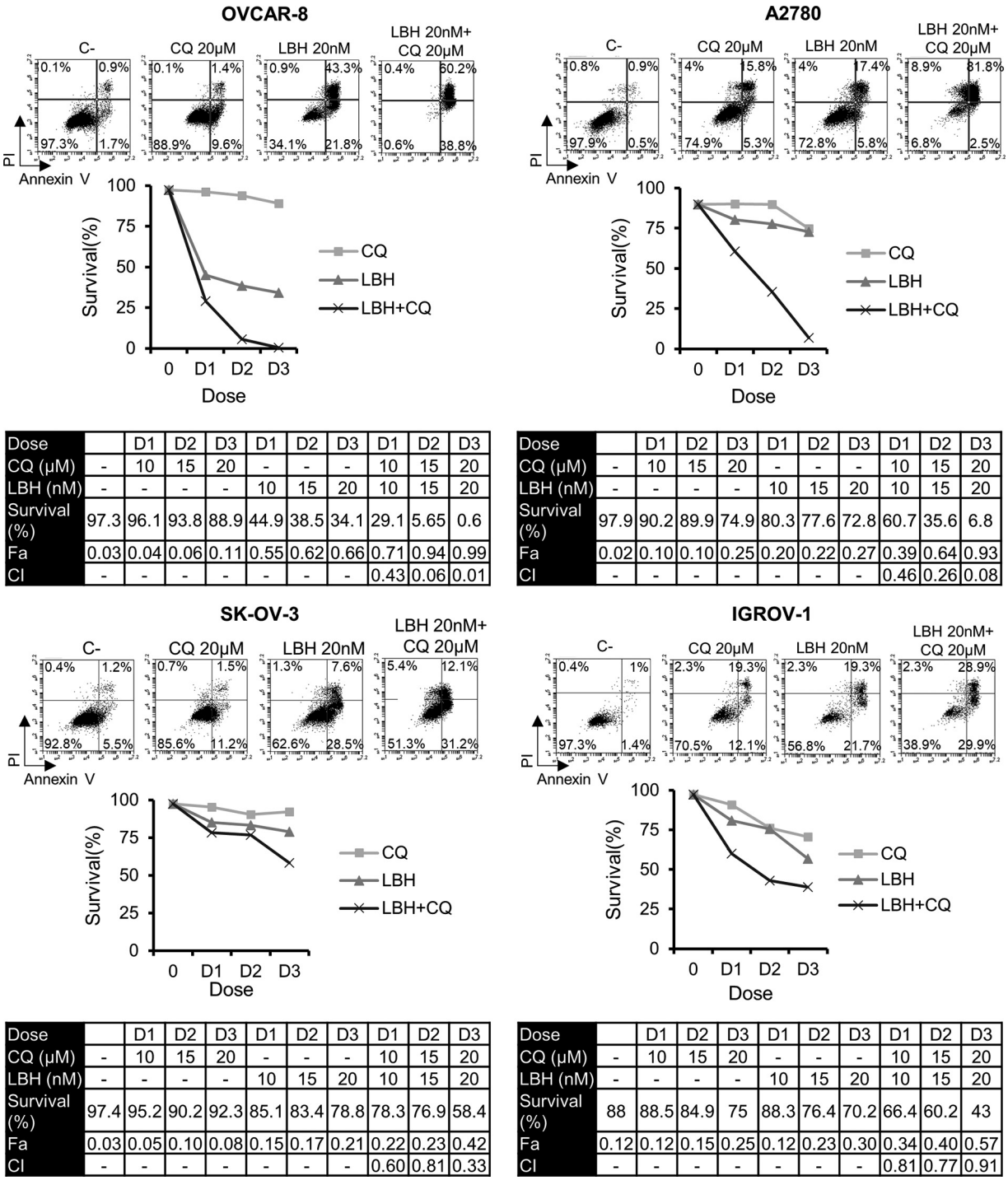

Dose		D1	D2	D3	D1	D2	D3	D1	D2	D3
CQ (μM)	-	10	15	20	-	-	-	10	15	20
LBH (nM)	-	-	-	-	10	15	20	10	15	20
Survival (%)	97.3	96.1	93.8	88.9	44.9	38.5	34.1	29.1	5.65	0.6
Fa	0.03	0.04	0.06	0.11	0.55	0.62	0.66	0.71	0.94	0.99
CI	-	-	-	-	-	-	-	0.43	0.06	0.01

Dose		D1	D2	D3	D1	D2	D3	D1	D2	D3
CQ (μM)	-	10	15	20	-	-	-	10	15	20
LBH (nM)	-	-	-	-	10	15	20	10	15	20
Survival (%)	97.9	90.2	89.9	74.9	80.3	77.6	72.8	60.7	35.6	6.8
Fa	0.02	0.10	0.10	0.25	0.20	0.22	0.27	0.39	0.64	0.93
CI	-	-	-	-	-	-	-	0.46	0.26	0.08

Dose		D1	D2	D3	D1	D2	D3	D1	D2	D3
CQ (μM)	-	10	15	20	-	-	-	10	15	20
LBH (nM)	-	-	-	-	10	15	20	10	15	20
Survival (%)	97.4	95.2	90.2	92.3	85.1	83.4	78.8	78.3	76.9	58.4
Fa	0.03	0.05	0.10	0.08	0.15	0.17	0.21	0.22	0.23	0.42
CI	-	-	-	-	-	-	-	0.60	0.81	0.33

Dose		D1	D2	D3	D1	D2	D3	D1	D2	D3
CQ (μM)	-	10	15	20	-	-	-	10	15	20
LBH (nM)	-	-	-	-	10	15	20	10	15	20
Survival (%)	88	88.5	84.9	75	88.3	76.4	70.2	66.4	60.2	43
Fa	0.12	0.12	0.15	0.25	0.12	0.23	0.30	0.34	0.40	0.57
CI	-	-	-	-	-	-	-	0.81	0.77	0.91

Fig. 3. Synergistic effect of the co-treatment with Panobinostat and chloroquine in OCCLs. Cells were exposed for 72 h to the indicated concentrations of LBH and CQ at a constant ratio and the percentage of apoptotic cells were assessed by flow cytometry (after cell staining with annexin V and propidium iodide). CI values less than 1 indicated a synergistic effect. These values were calculated using Compusyn Software. C-: negative control (untreated cells).

of these drugs for different times, stained with DCFH-DA, and analyzed by flow cytometry. A rapid induction of ROS was observed after treatment with CQ in all the OCCLs, in agreement with previous reports [35] (Fig. 4A). This induction was not observed when cells were cotreated with CQ and the antioxidant NAC. On the other hand, LBH did not increase ROS at short time; therefore, we analyzed its effect at longer treatment. After 24 h of treatment, we found that LBH increased ROS production in all the OCCLs except for A2780. The combination of CQ and LBH also induced ROS and the effect was stronger than the individual drugs in OVCAR-8 (Fig. 4A).

To analyze the relevance of ROS production in CQ/LBH-induced cell death we compared the viability of ovarian cells that had been incubated with these drugs (alone or in combination) in the presence or absence of the ROS scavenger NAC. Addition of the antioxidant reduced CQ-induced cell death in the most sensitive cell line A2780 but did not significantly decrease

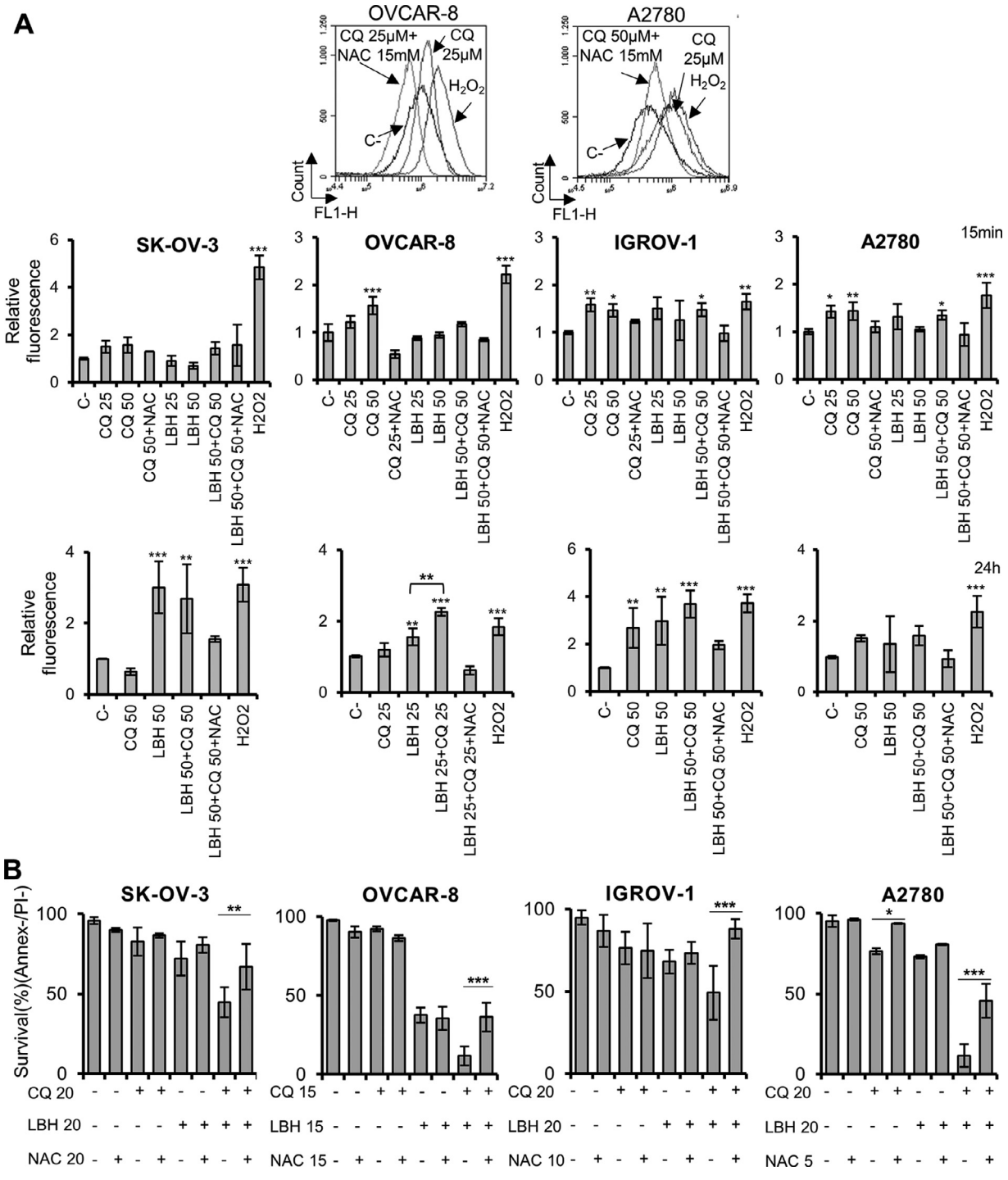

Fig. 4. Induction of ROS after treatment with CQ and LBH in OCCLs and effect in CQ/LBH-induced lethality. (A) Top panel, representative figures of ROS production after 15 min of treatment with the indicated concentrations of CQ (μM). The ROS increase was reverted by the addition of NAC (15 mM). Middle panel, ROS production after 15 min of treatment with the indicated concentrations of CQ (μM), LBH (nM) or NAC (mM). Bottom panel, ROS production after 24 h of treatment with the indicated concentrations of LBH and/or CQ. In all cases, 15 min of H_2O_2 treatment (1 mM) was used as a positive control. Data are the mean of at least 3 independent experiments. Error bars represent the SD (***$P < 0.001$, **$P < 0.01$, and *$P < 0.05$, compared to C-, unless otherwise specified). (B) Cells were exposed for 72 h to the indicated concentrations of CQ (μM), LBH (nM) and ROS scavenger NAC (mM) and the percentage of apoptotic cells were measured after cell staining with annexin V and propidium iodide by flow cytometry. C-: Negative control (untreated cells). Data are the mean of at least 3 independent experiments. Error bars represent the SD (***$P < 0.001$, **$P < 0.01$, and *$P < 0.05$).

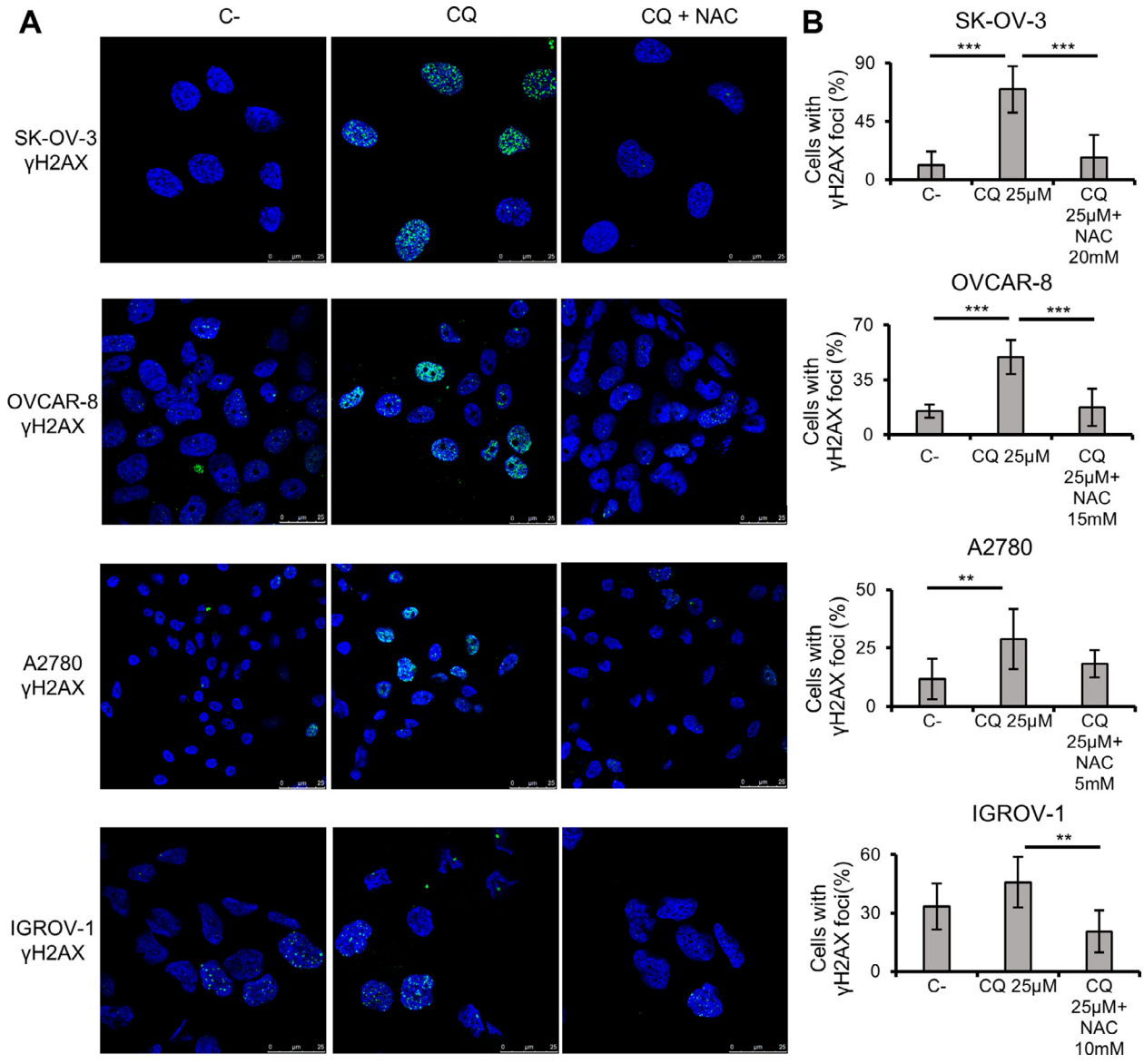

Fig. 5. CQ treatment induces DSBs that can be reverted by the addition of NAC in OCCLs. γH2AX foci were visualized by confocal microscopy and percentage of cells exhibiting γH2AX foci (>5 foci/cell) in the presence of CQ, NAC or both were calculated. A2780 and OVCAR-8 were treated for 48 h and IGROV-1 and SK-OV-3 for 72 h. C-: negative control (untreated cells). Data are the mean of the analysis of at least 50 cells per cell line. Error bars represent the SD (***$P < 0.001$, **$P < 0.01$, and *$P < 0.05$).

LBH-induced cell death in any of the 4 OCCLs analyzed (Fig. 4B). On the other hand, the presence of NAC clearly reduced the apoptosis induced by the combination of CQ and LBH in all 4 OCCLs.

Chloroquine induces DNA double-strand breaks (DSBs) in OCCLs that can be reverted by the addition of N-Acetylcysteine

ROS is a known generator of endogenous DNA damage, including DSBs, the most lethal of DNA lesions [42,43]. To analyze whether CQ and/or LBH induced DSBs in ovarian cells we monitored the phosphorylation of H2AX (γH2AX), a sensitive marker of DSBs, by immunofluorescence. CQ was found to induce DSBs in the 4 OCCLs analyzed (Fig. 5A). Addition of NAC decreased the percentage of cells with γH2AX foci, which clearly indicate that CQ-induced DSBs are caused by ROS (Fig. 5A and 5B). LBH significantly increased the number of cells with γH2AX foci in SK-OV-3 and OVCAR-8, but differing from the results obtained with CQ, foci numbers were not reduced in the presence of NAC. We observed that in the presence of LBH γH2AX foci were bigger than in untreated cells and also than those induced by CQ, especially in SKOV-3 and OVCAR-8 (Fig. 6A). These foci resemble persistent/irreparable DNA damage foci and could represent lesions especially difficult to repair [44].

Panobinostat inhibits homologous recombination repair (HR) in OCCLs

It has been described that some HDACi affect DNA DSB repair by inhibiting homologous recombination (HR) [12,13,16]. This data, together with the LBH-induced γH2AX foci appearance led us to the hypothesis that this HDAC inhibitor could also affect DSB repair by HR in OCCLs. Moreover, we also hypothesized that the synergy between CQ and LBH could be due to the induction of DSBs by CQ and the inhibition of

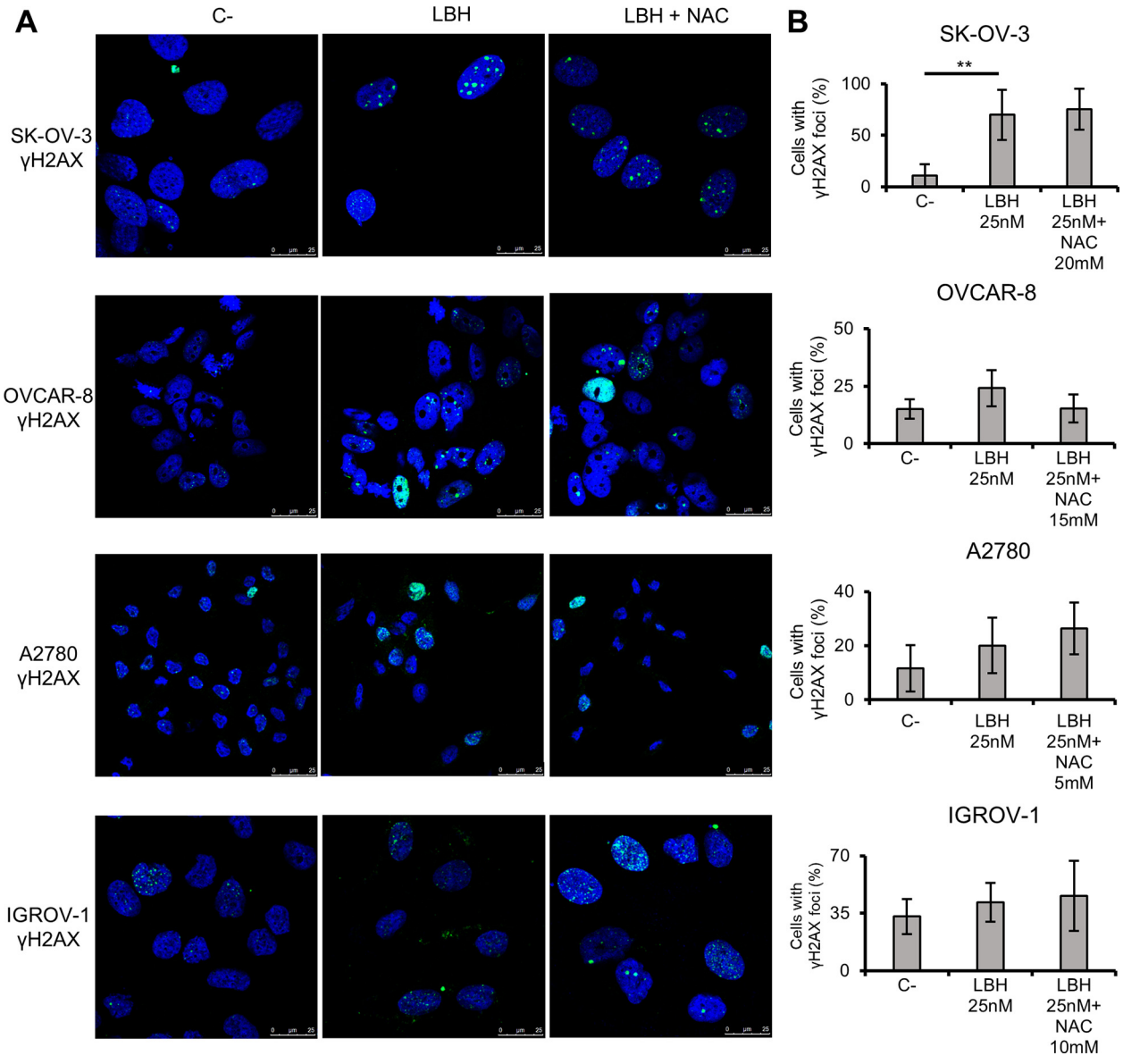

Fig. 6. Panobinostat induces DSBs which cannot be reverted by the addition of NAC in OCCLs. γH2AX foci were visualized by confocal microscopy and percentage of cells exhibiting γH2AX foci (>5 foci/cell) in the presence of LBH, NAC or both were calculated. A2780 and OVCAR-8 were treated for 48 h and IGROV-1 and SK-OV-3 for 72 h. C-: negative control (untreated cells). Data are the mean of the analysis of at least 50 cells per cell line. Error bars represent the SD ($^{***}P < 0.001$, $^{**}P < 0.01$, and $^{*}P < 0.05$).

their repair by LBH. To test these hypotheses, we measured HR efficiency in the presence of LBH in a multiple myeloma cell line that carries a chromosomally integrated GFP HR reporter cassette (JJN3-HR). This cell line has been proved in previous studies to be an optimal system to measure HR [12,45]. Cells were pretreated with LBH for 24 h, cotransfected with an *I-SceI* endonuclease-expressing plasmid and a pDsRed-N1 plasmid (red), to normalize for transfection efficiency, and incubated again for an additional 48 h. In this system, correct repair by HR of DSBs induced by the endonuclease restored a functional GFP detectable by flow cytometry (green cells). Mirin, an inhibitor of MRN complex (Mre11-Rad51-Nsb1) required for HR, was used as a control [45]. Using this system, we found a significant reduction in the number of HR-proficient cells that had been treated with LBH compared with untreated cells (Fig. 7A). To corroborate these findings in ovarian cells, we then generated an ovarian cancer cell line carrying the HR GFP reporter cassette (SK-OV-3-HR). We also found a significant reduction in HR efficiency after the treatment with LBH (Fig. 7B).

Panobinostat inhibits the correct recruitment of Rad51 protein to DSBs

We and other researchers have previously shown that some HDAC inhibitors decrease Rad51 levels or affect the recruitment of Rad51 to DSB sites [12–14,46,47]. Therefore, we next analyzed the localization of Rad51 in OCCLs treated with LBH, CQ or both. Cells were also stained with antiγH2AX to mark DSB sites. In the SK-OV-3 cell line CQ-treated cells showed γH2AX that colocalized with Rad51 foci, as expected; however, LBH-treated cells exhibited clear γH2AX but no Rad51 foci was observed. In the case of OVCAR-8, Rad51 staining after treatment with LBH revealed that the protein was localized in the cytoplasm and in the nucleoli (Fig. 8).

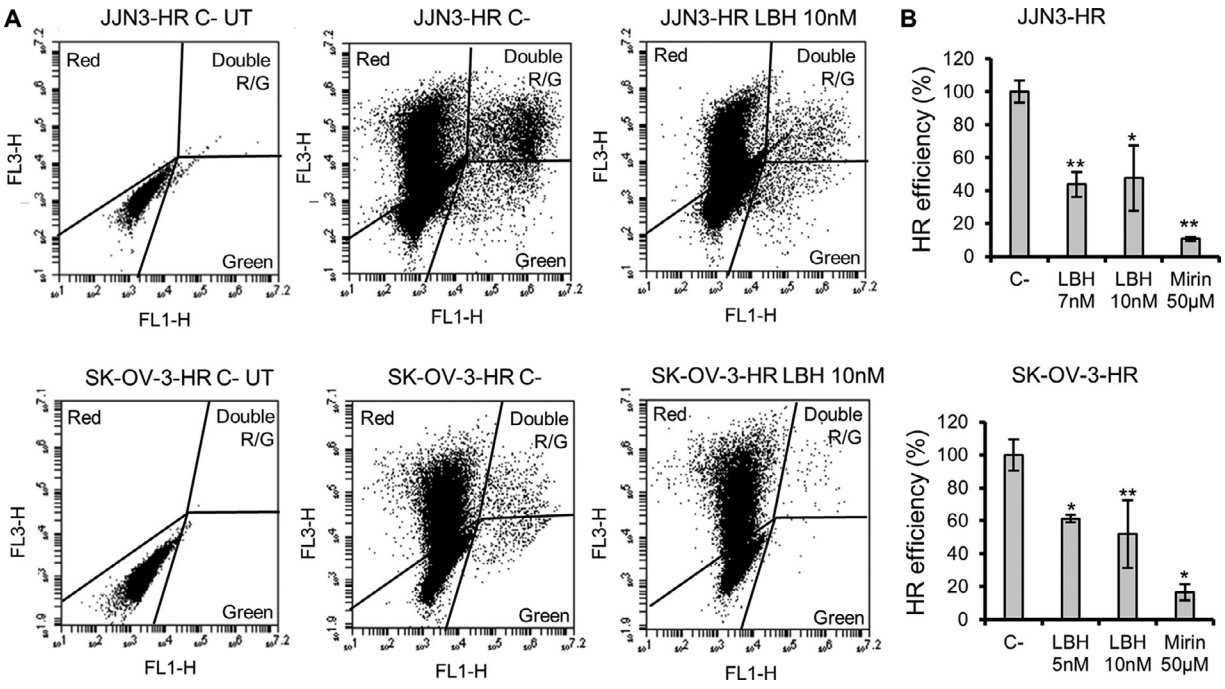

Fig. 7. Panobinostat inhibits DSB repair by homologous recombination. (A) JJN3-HR and SK-OV-3-HR cells were pre-treated or not (C-) with LBH for 24 h and then co-transfected or not (UT) with 5 μg of an I-SceI endonuclease-expressing plasmid and 0.5 μg of pDsRed2-N1 (red cells) and incubated in the presence or absence (C-) of LBH for additional 48 h. Correct HR repair restored GFP gene that was detected as green cells. 15000 DsRed+ are shown in both cell lines. (B) HR efficiency calculated as the ratio of GFP+ to DsRed+ cells. Data are the mean of 3 independent experiments. Error bars represent the SD ($^{**}P < 0.01$, $^{*}P < 0.05$).

Combination of Mirin and Chloroquine synergistically induces cell death in OCCLs

To further support the hypothesis that the synergy between CQ and LBH could be due to the induction of DSBs by CQ and the inhibition of their repair by LBH, we studied whether treatment with a well-known HR inhibitor, Mirin, together with CQ also produced a synergistic effect. We found that compared to monotherapy treatment, cell viability was lower when the combination of Mirin and CQ was used in the 4 OCCLs (Figure S5A). When the CIs was calculated a synergistic effect between these 2 drugs was found in A2780, SK-OV-3 and IGROV-1 (CI<1).

Combination of bafilomycin A1 and Panobinostat synergistically induces cell death in OCCLs

It had been previously described that the use of autophagy inhibitors, such as CQ, with drugs that induces autophagy, such as HDACi, enhanced the cytotoxic response of these drugs [18–23,48]. Therefore, we hypothesized that the synergistic effect obtained after CQ/LBH cotreatment could also be due, at least in part, to an inhibition of the prosurvival autophagy pathway. To test this hypothesis, we next studied whether the use of another autophagy inhibitor, bafilomycin A1, could also enhance the LBH cytotoxic effect. We compared the effect of the combination of bafilomycin A1 and LBH with the effect of these agents in monotherapy and found that cell viability was lower when the combination was used in OVCAR-8, SK-OV-3 and IGROV-1 cell lines. To determine a potential synergistic effect, combination indices were calculated. A synergistic effect between these 2 drugs was found in the OVCAR-8, SK-OV-3, and IGROV-1 cell lines (CI<1). The strongest synergism was found in SK-OV-3 cell line (CI<0.5) (Figure S5B).

Discussion

The combination of 2 or more therapeutic treatments is a cornerstone of cancer therapy [49]. The idea is to find drug combinations that work in an additive, or better, in a synergistic manner, that is, when the effect of 2 or more agents working in combination is greater than the expected additive effect [50]. These approaches increase the potential to overcome drug resistance by targeting nonoverlapping signaling pathways and allow a lower therapeutic dosage of each individual drug, which reduces toxicity. The development of combinational therapies is especially important for the treatment of cancers with high mortality rate, such as ovarian cancer. Here, we describe for the first time that treatment with an HDACi, LBH, and CQ exerts a strong synergistic effect in ovarian cancer cells and analyzed the causes of the observed synergism. We show that CQ induces the production of ROS causing DNA DSBs, whereas LBH inhibits the repair of these lesions by HR, providing an explanation for the observed synergism.

A previous study has reported a synergistic effect between LBH and CQ in breast cancer cell lines [19]. The authors showed that exposure to LBH increased LC3B-II but reduced the levels of p62, consistent with the degradation of p62 during LBH-induced autophagic flux [51,52]. This data, that was also observed in the present work with OCCLs, led the authors to the hypothesis that LBH-treated cells would be particularly dependent on autophagy for survival, making them more susceptible to inhibition of autophagy by CQ, which inhibits autophagy, thereby increasing levels of p62 and LC3B-II [19,53]. These effects of CQ on p62 and LC3B-II levels were also observed in all the OCCLs analyzed in the present study, as well as a clear accumulation of autophagosomes. Other reports have also shown that CQ enhances the *in vitro* and *in vivo* efficacy of some HDACis; thus, in colon cancer cells, treatment with CQ or knockdown of the essential autophagy gene *ATG7* sensitized cells to vorinostat-induced apoptosis [18] and in chronic myeloid leukemia (CML) cells treatment with drugs that disrupt

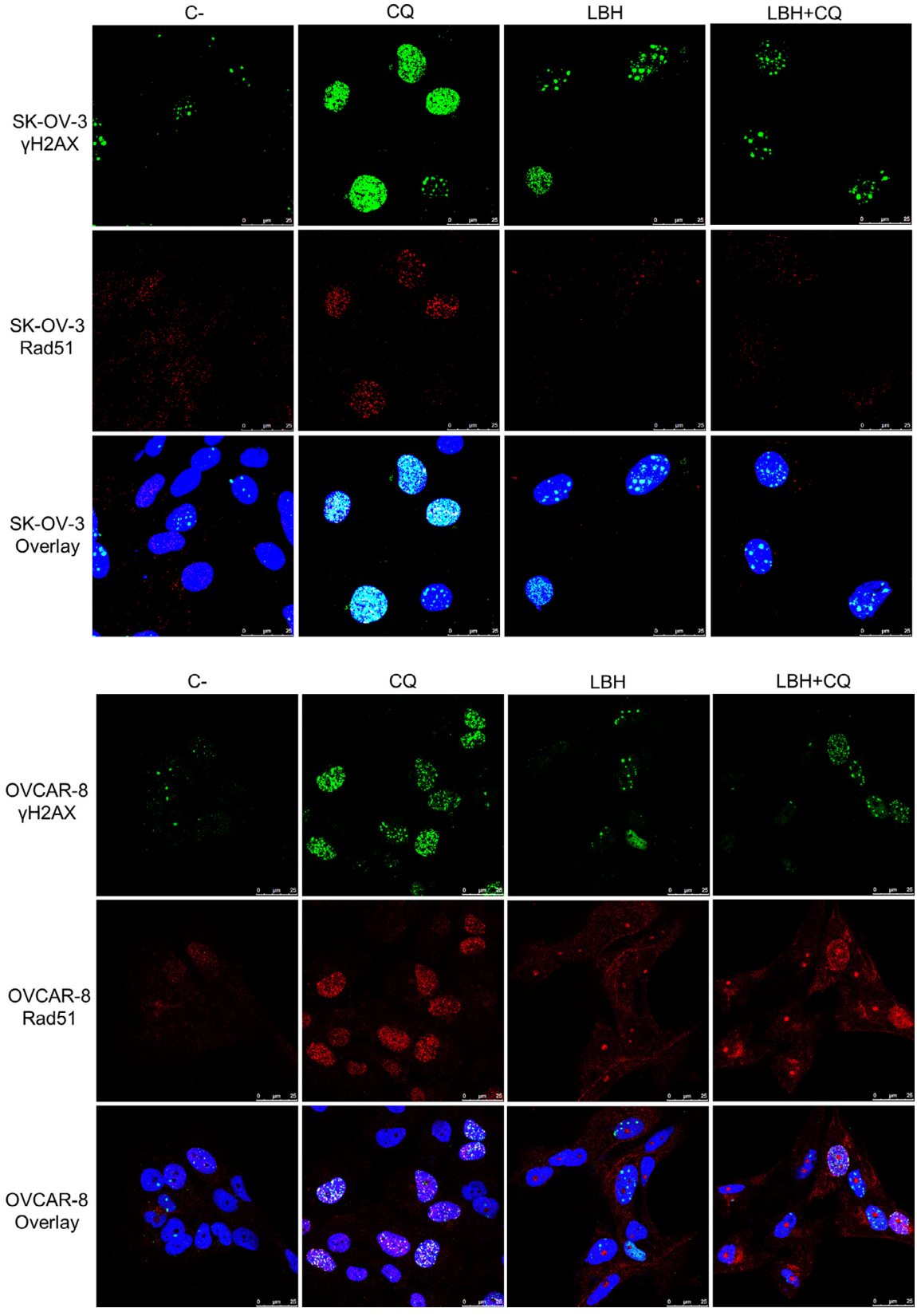

Fig. 8. Effect of Panobinostat treatment in the correct recruitment of Rad51 protein to DSBs. Immunofluorescence of SK-OV-3 and OVCAR-8 cell lines for γH2AX and Rad51 foci detection after 48 h (OVCAR-8) or 72 h (SK-OV-3) of treatment with 25 μM of CQ, 25 nM of LBH or both. C-: negative control (untreated cells).

the autophagy pathway dramatically increase the antineoplastic effects of SAHA [20]. However, the fact that HDACi-induced autophagy serves as a survival mechanism that is avoided by CQ or other autophagy inhibitors remains controversial, since other reports have shown the opposite effect. For example, Liu et al described that in hepatocellular carcinoma SAHA-induced cytotoxicity was inhibited by 3-methyladenine or *ATG5* knockout, which inhibits autophagy, indicating that SAHA-induced autophagy led to cell death [32]. Similarly, Yamamoto et al. also described that SAHA-induced cell death could be reverted using 3-methyladenine [54]. It has also been reported that CQ sensitizes some cancer cells to chemotherapy independently of autophagy. Thus, Maycotte et al described that CQ, but not autophagy blockage by knocking out autophagy genes such as *ATG12* and *BECN1* or treatment with the autophagy inhibitor Bafilomycin A1, increased the sensitivity of breast cancer cells to chemotherapy [27]. To try to elucidate if autophagy serves as a survival mechanism in HDACi-treated cells, we decided to investigate the cytotoxic effect of the combination of LBH and another inhibitor of autophagy, Bafilomycin A1. We did observe a synergistic effect in 3 out of 4 OCCLs analyzed, which suggest that the regulation of autophagy may contribute to the efficacy of the combination. In this regard, several reports have previously shown the relevance of autophagy inhibition as a therapeutic option in ovarian carcinoma, since treatment with chemotherapeutic drugs, such as cisplatin or paclitaxel, upregulates autophagy which contributes to chemotherapy resistance [55]. However, we did not find a synergistic effect in A2780 cell line treated with LBH and Bafilomycin A1. This result, and the discrepancies among different reports mentioned above, could be due to differences in cancer cell lines or HDAC inhibitors but reveal that some CQ/HDACi autophagy-independent effects must contribute to the described synergistic interactions. In the case of A2780, induction of autophagy by LBH could be lower than in the rest of the cell lines analyzed, in fact, we did not observe p62 degradation, therefore CQ/LBH synergy may attempt to another mechanism. In this regard, CQ and also HDACi have been described to induce pleiotropic effects on cells [6,10,29,56,11–15,25,27,28].

To investigate the underlying causes of synergism between CQ and LBH we have used 4 different OCCLs representing the most common histopathological OC subtypes (high-grade serous, endometrioid and clear cell ovarian carcinomas). A2780 and IGROV-1 cell lines were derived from ovarian endometrioid adenocarcinomas and represent this subtype of OC; in fact, IGROV-1 cells present a mixed histology harboring molecular alterations typical of clear cells and endometrioid subtypes. OVCAR-8 and SK-OV-3 cell lines were obtained from high-grade serous adenocarcinomas and ascites from a serous cystadenoma, respectively. We first analyzed the individual effect of the drugs under study. We show that CQ inhibited proliferation, in agreement with previous reports [40,57]. However, it did not affect cell cycle profile, as also found Carew et al [20], but in contrast with other authors reporting a G0/G1 arrest [57]. We also found that CQ increases ROS, as previously reported in different cancer cell lines [18,20,35–37,40,57,58], and this effect resulted in the formation of DSBs in ovarian cells, since the presence of the antioxidant NAC completely restored the number of cells with endogenous γH2AX foci. Our data show that CQ induces ROS in OCCLs as soon as 15 min after treatment. These species were reduced at 24 h in OCCLs with the exception of IGROV-1, in agreement with previous reports [35]. The mechanisms that promote ROS induction and the impact of DNA lesions to induce cell death has not been deeply investigated, but it has been described that autophagy might prevents ROS accumulation through elimination of damaged mitochondria, which are known to be the major source of ROS [41]. Therefore, autophagy blockage induced by CQ might be the cause of increased ROS leading to DNA damage. Alternatively, it has been suggested that the increased permeability of mitochondrial membrane by cathepsins, liberated from lysosome after the lysosomal membrane permeabilization produced by CQ, may be responsible for ROS generation [20,40]. The slight effect of CQ in the induction of apoptosis in OCCLs probably attempts to an efficient DSB repair in the OCCLs analyzed. On the other hand, we did not detect a significant increase in ROS after the treatment with LBH at short time; however, we detected a significant induction of ROS at longer time (24 h) in 3 of the 4 cell lines analyzed. After 24 h of cotreatment with both agents, anincrease in ROS production was detected in the 4 OCCLs compared to untreated cells, and this increase was higher than those obtained after LBH treatment alone in OVCAR-8. These results are consistent with those reported in previous studies in colon cancer cells [18] and hematological tumor cells, where different HDACi were found to induce ROS [59,60]. ROS generation could explain the increase in the percentage of cells with γH2AX foci after treatment with LBH. However, the percentage of cells with γH2AX foci was not significantly reduced by the addition of ROS scavenger NAC. These results suggest that LBH could affect some DNA repair pathways, such as HR, that might avoid a correct repair of DSBs. In fact, we found that LBH significantly decreased the efficiency of HR, and this must depend, at least in part, on an improper recruitment of Rad51 recombinase to DSB sites, as revealed the immunofluorescence assays. These results are consistent with previous reports using other HDACi [12–14,46,47]. Other researchers have also described defects in ATM signaling after treatment with HDACi [15], if that is also the case in OCCLs requires further investigation. To further support the hypothesis that CQ induce DSBs and LBH avoids their repair, we analyzed the effect of the combination of CQ and a well-known HR inhibitor, Mirin. We found that this combination also exerted a synergistic effect in 3 out of 4 cell lines analyzed, which again confirms that inhibition of HR enhances the efficacy of the DSB-inducer CQ. Moreover, we found that NAC protects against CQ/LBH-induced cell death, revealing that the cytotoxic effect of the double combination is, at least in part, due to the generation of DSBs by oxidative stress.

Conclusions

Altogether, our results strongly suggest that induction of DNA damage and inhibition of DNA repair play an important role in CQ/LBH-induced cell death and explain, together with the modulation of autophagy, the strong synergy observed after treatment with these 2 drugs.

Interestingly, the combination of LBH and CQ has been shown to reduced tumor formation in breast xenografts *in vivo* with low cytotoxicity [19]. These results, together with our findings in 4 OCCLs that represent different types of ovarian carcinomas, indicate that CQ plus LBH must be considered for the treatment of several cancers and therefore investigated in clinical trials.

Author contributions

Conceptualization, AB.H. and R.G.-S.; methodology, M.O.-S and AB.H.; validation, AB.H, and R.G.-S.; formal analysis, M.O.-S.; investigation, AB.H. and M.O.-S; resources, R.G.-S.; data curation, M.O.-S.; writing—original draft preparation, M.O.-S, AB.H.; writing—review and editing, M.O.-S, AB.H and R.G.-S; visualization, M.O.-S, AB.H, R.G.-S; supervision, AB.H and R.G.-S; project administration, R.G.-S.; funding acquisition, R.G.-S. All authors have read and agreed to the published version of the manuscript.

Funding

This study was supported by the health research program of the "Instituto de Salud Carlos III" (Spanish Ministry of Economy and Competitiveness, PI16/01920 and PI20/01569) co-funded with FEDER founds and project CSI264P20 ("Consejería de Educación de la Junta de Castilla y León"). M.O.-S was supported by a predoctoral research grant from the Institute of Biomedical Research of Salamanca (IBSAL) (IBpredoc17/00010).

Acknowledgments

The authors thank to the Microscopy and Cytometry Unit from the Institute of Molecular and Cellular Biology of Cancer (IBMCC) for their technical assistance.

Supplementary materials

Supplementary material associated with this article can be found, in the online version, at doi:10.1016/j.neo.2021.04.003.

References

[1] Bray F, Ferlay J, Soerjomataram I, Siegel RL, Torre LA, Jemal A. Global cancer statistics 2018: GLOBOCAN estimates of incidence and mortality worldwide for 36 cancers in 185 countries. *CA Cancer J Clin* 2018 Nov 1;**68**(6):394–424.

[2] Lheureux S, Gourley C, Vergote I, Oza AM. Epithelial ovarian cancer. In: The Lancet, Vol. 393. Lancet Publishing Group; 2019. p. 1240–53.

[3] Giornelli GH. Management of relapsed ovarian cancer: a review. *Springerplus* 2016;**5**(1197).

[4] Van Zyl B, Tang D, Bowden NA. Biomarkers of platinum resistance in ovarian cancer: What can we use to improve treatment. *Endocr Relat Cancer* 2018;**25**:R303–18.

[5] Pokhriyal R, Hariprasad R, Kumar L, Hariprasad G. Chemotherapy resistance in advanced ovarian cancer patients. *Biomark Cancer* 2019:11.

[6] Eckschlager T, Plch J, Stiborova M, Hrabeta J. Histone deacetylase inhibitors as anticancer drugs. *Int J Mol Sci* 2017;**18**(7).

[7] Suraweera A, O'Byrne KJ, Richard DJ. Combination therapy with histone deacetylase inhibitors (HDACi) for the treatment of cancer: Achieving the full therapeutic potential of HDACi. *Front Oncol* 2018;**8**.

[8] Ropero S, Esteller M. The role of histone deacetylases (HDACs) in human cancer. *Mol Oncol* 2007;**1**:19–25.

[9] Kim TY, Bang YJ, Robertson KD. Histone deacetylase inhibitors for cancer therapy. *Epigenetics* 2006;**1**(1):15–24.

[10] Newbold A, Falkenberg KJ, Prince HM, Johnstone RW. How do tumor cells respond to HDAC inhibition? *FEBS J* 2016;**283**:4032–46.

[11] Bolden JE, Peart MJ, Johnstone RW. Anticancer activities of histone deacetylase inhibitors. *Nat Rev Drug Discov* 2006;**5**:769–84.

[12] López-Iglesias AA, Herrero AB, Chesi M, San-Segundo L, González-Méndez L, Hernández-García S, Misiewicz-Krzeminska I, Quwaider D, Martín-Sánchez M, Primo D, et al. Preclinical anti-myeloma activity of EDO-S101, a new bendamustine-derived molecule with added HDACi activity, through potent DNA damage induction and impairment of DNA repair. *J Hematol Oncol* 2017;**10**(1):1–14.

[13] Wilson AJ, Sarfo-Kantanka K, Barrack T, Steck A, Saskowski J, Crispens MA, Khabele D. Panobinostat sensitizes cyclin E high, homologous recombination-proficient ovarian cancer to olaparib. *Gynecol Oncol* 2016;**143**(1):143–51.

[14] Adimoolam S, Sirisawad M, Chen J, Thiemann P, Ford JM, Buggy JJ. HDAC inhibitor PCI-24781 decreases RAD51 expression and inhibits homologous recombination. *Proc Natl Acad Sci U S A.* 2007;**104**:19482–7.

[15] Thurn KT, Thomas S, Raha P, Qureshi I, Munster PN. Histone deacetylase regulation of ATM-mediated DNA damage signaling. *Mol Cancer Ther* 2013;**12**:2078–87.

[16] de Andrade PV, Andrade AF, de Paula, Queiroz RG, Scrideli CA, Tone LG, Valera ET. The histone deacetylase inhibitor PCI-24781 as a putative radiosensitizer in pediatric glioblastoma cell lines. *Cancer Cell Int* 2016;**16**(1):31.

[17] Bishop E, Bradshaw TD. Autophagy modulation: a prudent approach in cancer treatment? *Cancer Chemother Pharmacol* 2018;**82**:913–22.

[18] Carew JS, Medina EC, Esquivel JA, Mahalingam D, Swords R, Kelly K, Zhang H, Mita AC, Mita MM, Giles JF, et al. Autophagy inhibition enhances vorinostat-induced apoptosis via ubiquitinated protein accumulation. *J Cell Mol Med* 2010;**14**:2448–59.

[19] Rao R, Balusu R, Fiskus W, Mudunuru U, Venkannagari S, Chauhan L, et al. Combination of pan-histone deacetylase inhibitor and autophagy inhibitor exerts superior efficacy against triple-negative human breast cancer cells. *Mol Cancer Ther* 2012;**11**(4):973–83.

[20] Carew JS, Nawrocki ST, Kahue CN, Zhang H, Yang C, Chung L, et al. Targeting autophagy augments the anticancer activity of the histone deacetylase inhibitor SAHA to overcome Bcr-Abl-mediated drug resistance. *Blood* 2007;**110**:313–22.

[21] Gao L, Sun X, Zhang Q, Chen X, Zhao T, Lu L, Zhang J, Hong Y. Histone deacetylase inhibitor trichostatin a and autophagy inhibitor chloroquine synergistically exert anti-tumor activity in H-ras transformed breast epithelial cells. *Mol Med Rep* 2018;**17**:4345–50.

[22] Kommalapati VK, Kumar D, Tangutur AD. Inhibition of JNJ-26481585-mediated autophagy induces apoptosis via ROS activation and mitochondrial membrane potential disruption in neuroblastoma cells. *Mol Cell Biochem* 2020 Mar 7;**468**(1–2):21–34.

[23] Torgersen ML, Engedal N, Bøe SO, Hokland P, Simonsen A. Targeting autophagy potentiates the apoptotic effect of histone deacetylase inhibitors in t(8;21) AML cells. *Blood* 2013 Oct 3;**122**(14):2467–76.

[24] AA Al-Bari. Chloroquine analogues in drug discovery: New directions of uses, mechanisms of actions and toxic manifestations from malaria to multifarious diseases. *J Antimicrob Chemother* 2014;**70**:1608–21.

[25] Mauthe M, Orhon I, Rocchi C, Zhou X, Luhr M, Hijlkema KJ, Coppes RP, Engedal N, Mari M, Reggiori F. Chloroquine inhibits autophagic flux by decreasing autophagosome-lysosome fusion. *Autophagy* 2018;**14**(8):1435–55.

[26] Verbaanderd C, Maes H, Schaaf MB, Sukhatme VP, Pantziarka P, Sukhatme V, Agostinis P, Bouche G. Repurposing drugs in oncology (ReDO) - Chloroquine and hydroxychloroquine as anti-cancer agents. *Ecancermedicalscience* 2017;**11**:781. PMID: 29225688; PMCID: PMC5718030. doi:10.3332/ecancer.2017.781.

[27] Maycotte P, Aryal S, Cummings CT, Thorburn J, Morgan MJ, Thorburn A. Chloroquine sensitizes breast cancer cells to chemotherapy independent of autophagy. *Autophagy* 2012;**8**.

[28] Eng CH, Wang Z, Tkach D, Toral-Barza L, Ugwonali S, Liu S, Fitzgerald SL, George E, Frías E, Cochran N, et al. Macroautophagy is dispensable for growth of KRAS mutant tumors and chloroquine efficacy. *Proc Natl Acad Sci U S A* 2016;**113**:182–7.

[29] Enzenmüller S, Gonzalez P, Debatin KM, Fulda S. Chloroquine overcomes resistance of lung carcinoma cells to the dual PI3K/mTOR inhibitor PI103 by lysosome-mediated apoptosis. *Anticancer Drugs* 2013;**24**:14–19.

[30] Mao Z, Bozzella M, Seluanov A, Gorbunova V. Comparison of nonhomologous end joining and homologous recombination in human cells. *DNA Repair (Amst)* 2008;**7**:1765–71.

[31] Gammoh N, Lam D, Puente C, Ganley I, Marks PA, Jiang X. Role of autophagy in histone deacetylase inhibitor-induced apoptotic and nonapoptotic cell death. *Proc Natl Acad Sci U S A.* 2012 Apr 24;**109**(17):6561–5.

[32] Liu YL, Yang PM, Shun CT, Wu MS, Weng JR, Chen CC. Autophagy potentiates the anti-cancer effects of the histone deacetylase inhibitors in hepatocellular carcinoma. *Autophagy* 2010;**6**(8):1057–65.

[33] Shao Y, Gao Z, Marks PA, Jiang X. Apoptotic and autophagic cell death induced by histone deacetylase inhibitors. *Proc Natl Acad Sci U S A.* 2004;**101**(52):18030–5.

[34] Chiu HW, Yeh YL, Ho SY, Wu YH, Wang BJ, Huang WJ, Ho YS, Wang YJ, Chen LC, Tu SH. A new histone deacetylase inhibitor enhances radiation sensitivity through the induction of misfolded protein aggregation and autophagy in triple-negative breast cancer. *Cancers (Basel)* 2019;**11**(11).

[35] Pare J, Choi K, Jeong E, Kwon D, Benveniste EN, Choi C. Reactive oxygen species mediate chloroquine-induced expression of chemokines by human astroglial cells. *Glia* 2004;**47**(1):9–20.

[36] Qu X, Sheng J, Shen L, Su J, Xu Y, Xie Q, Wu Y, Zhang X, Sun L. Autophagy inhibitor chloroquine increases sensitivity to cisplatin in QBC939 cholangiocarcinoma cells by mitochondrial ROS. *PLoS One* 2017;**12**(3).

[37] Ganguli A, Choudhury D, Datta S, Bhattacharya S, Chakrabarti G . Inhibition of autophagy by chloroquine potentiates synergistically anti-cancer property of artemisinin by promoting ROS dependent apoptosis. *Biochimie* 2014;**107**(PB):338–49.

[38] Rosato RR, Almenara JA, Maggio SC, Coe S, Atadja P, Dent P, Grant S. Role of histone deacetylase inhibitor-induced reactive oxygen species and DNA damage in LAQ-824/fludarabine antileukemic interactions. *Mol Cancer Ther* 2008;**7**(10):3285–97.

[39] Ruefli AA, Ausserlechner MJ, Bernhard D, Sutton VR, Tainton KM, Kofler R, Smyth MJ, Johnstone RW. The histone deacetylase inhibitor and chemotherapeutic agent suberoylanilide hydroxamic acid (SAHA) induces a cell-death pathway characterized by cleavage of Bid and production of reactive oxygen species. *Proc Natl Acad Sci U S A.* 2001;**98**(19):10833–8.

[40] Park D, Lee Y. Biphasic activity of Chloroquine in human colorectal cancer cells. *Dev Reprod* 2014;**18**:225–31.

[41] Poillet-Perez L, Despouy G, Delage-Mourroux R, Boyer-Guittaut M. Interplay between ROS and autophagy in cancer cells, from tumor initiation to cancer therapy. *Redox Biol* 2015;**4**:184–92.

[42] Scott SP, Pandita TK. The cellular control of DNA double-strand breaks. *J Cell Biochem. NIH Public Access* 2006;**99**:1463–75.

[43] Srinivas US, Tan BWQ, Vellayappan BA, Jeyasekharan AD. *ROS and the DNA damage response in cancer*, Vol. 25. Redox Biology. Elsevier B.V.; 2019.

[44] Herrero AB, SanMiguel J, Gutierrez NC. Deregulation of DNA double-strand break repair in multiple myeloma: Implications for genome stability. *PLoS One* 2015 19;**10**(3).

[45] Herrero AB, Gutiérrez NC. Targeting ongoing DNA damage in multiple myeloma: Effects of DNA damage response inhibitors on plasma cell survival. *Front Oncol* 2017;**7**(MAY):98.

[46] Lai TH, Ewald B, Zecevic A, Liu C, Sulda M, Papaioannou D, Garzon R, Blachly JS, Plunkett W, Sampath D. HDAC Inhibition Induces MicroRNA-182, which Targets RAD51 and Impairs HR repair to sensitize cells to sapacitabine in acute myelogenous leukemia. *Clin Cancer Res* 2016;**22**(14):3537–49.

[47] Kachhap SK, Rosmus N, Collis SJ, Kortenhorst MSQ, Wissing MD, Hedayati M, Shabbeer S, Mendonca J, Deangelis J, Marchionni L, et al. Downregulation of homologous recombination DNA repair genes by HDAC inhibition in prostate cancer is mediated through the E2F1 transcription factor. *PLoS One* 2010;**5**(6).

[48] He G, Wang Y, Pang X, Zhang B. Inhibition of autophagy induced by TSA sensitizes colon cancer cell to radiation. *Tumor Biol* 2014;**35**:1003–11.

[49] Mokhtari RB, Homayouni TS, Baluch N, Morgatskaya E, Kumar S, Das B, Yeger H. Combination therapy in combating cancer. *Oncotarget* 2017;**8**:38022–43.

[50] Greco WR, Faessel H, Levasseur L. The search for cytotoxic synergy between anticancer agents: a case of Dorothy and the ruby slippers? *J Natl Cancer Inst* 1996;**88**:699–700.

[51] Moscat J, Diaz-Meco MT. p62 at the crossroads of autophagy, apoptosis, and cancer. *Cell.* 2009;**137**:1001–4.

[52] Komatsu M, Ichimura Y. Physiological significance of selective degradation of p62 by autophagy. *FEBS Lett* 2010;**584**:1374–8.

[53] Amaravadi RK, Lippincott-Schwartz J, Yin XM, Weiss WA, Takebe N, Timmer W, DiPaola RS, Lotze MT, White E. Principles and current strategies for targeting autophagy for cancer treatment. *Clin Cancer Res* 2011;**17**:654–66.

[54] Yamamoto S, Tanaka K, Sakimura R, Okada T, Nakamura T, Li Y, Takasaki M, Nakabeppu Y, Iwamoto Y. Suberoylanilide hydroxamic acid (SAHA) induces apoptosis or autophagy-associated cell death in chondrosarcoma cell lines. *Anticancer Res* 2008;**28**(3A):1585–91.

[55] Zhan L, Zhang Y, Wang W, Song E, Fan Y, Li J, Wei B. Autophagy as an emerging therapy target for ovarian carcinoma. *Oncotarget* 2016;**7**(50):83476–87.

[56] Shukla AM, Shukla AW. Expanding horizons for clinical applications of chloroquine, hydroxychloroquine, and related structural analogues. *Drugs Context* 2019;**8**.

[57] Hu T, Li P, Luo Z, Chen X, Zhang J, Wang C, Chen P, Dong Z. Chloroquine inhibits hepatocellular carcinoma cell growth in vitro and in vivo. *Oncol Rep* 2016;**35**:43–9.

[58] Farombi EO. Genotoxicity of chloroquine in rat liver cells: Protective role of free radical scavengers. *Cell Biol Toxicol* 2006;**22**:159–67.

[59] Pei XY, Dai Y, Grant S. Synergistic induction of oxidative injury and apoptosis in human multiple myeloma cells by the proteasome inhibitor bortezomib and histone deacetylase inhibitors. *Clin Cancer Res* 2004;**10**:3839–52.

[60] Rosato RR, Almenara JA, Grant S. The histone deacetylase inhibitor MS-275 promotes differentiation or apoptosis in human leukemia cells through a process regulated by generation of reactive oxygen species and induction of p21CIP1/WAF1. *Cancer Res* 2003;**63**(13):3637–45.